Evolutionary rescue model informs strategies for driving cancer cell populations to extinction

Amjad Dabi[1,*], Joel S. Brown[2,3], Robert A. Gatenby[2,3,4], Corbin D. Jones[5,6,7,*], and Daniel R. Schrider[1,7,*]

1. Department of Genetics, University of North Carolina, Chapel Hill, North Carolina, USA

2. Department of Cancer Biology and Evolution, Moffitt Cancer Center, Tampa, FL, USA

3. Department of Integrated Mathematical Oncology, Moffitt Cancer Center, Tampa, FL, USA

4. Diagnostic Imaging Department, Moffitt Cancer Center, Tampa, FL, USA

5. Department of Biology, University of North Carolina, Chapel Hill, North Carolina, USA

6. Integrative Program for Biological and Genome Sciences, University of North Carolina, Chapel Hill, North Carolina, USA

7. UNC Lineberger Comprehensive Cancer Center, University of North Carolina, Chapel Hill, North Carolina, USA

*corresponding authors: amjad_dabi@unc.edu, cdjones@email.unc.edu, drs@unc.edu

ABSTRACT

Cancers exhibit a remarkable ability to develop resistance to a range of treatments, often resulting in relapse following first-line therapies and significantly worse outcomes for subsequent treatments. While our understanding of the mechanisms and dynamics of the emergence of resistance during cancer therapy continues to advance, many questions remain about which treatment strategies can minimize the probability that resistance will evolve, thereby improving long-term patient outcomes. In this study, we present an evolutionary simulation model of a clonal population of cells that can acquire resistance mutations to one or more treatments. We then leverage this model to examine the efficacy of a two-strike "extinction therapy" protocol—in which two treatments are applied sequentially in an effort to first contract the population to a vulnerable state and then push it to extinction—in comparison to that of a combination therapy protocol. We investigate the impact of parameters such as the timing of the switch between the two strikes, the rate of emergence of resistant mutations, the dose of the applied drugs, the presence of cross-resistance, and whether resistance is a binary or a quantitative trait. Our results indicate that the timing of switching from the first to the second strike has a marked effect on the likelihood of driving the population to extinction, and that extinction therapy outperforms combination therapy when cross-resistance is present. We conduct an *in silico* trial that reveals more detailed insight into when and why a second strike will succeed or fail. Finally, we demonstrate that modeling resistance as a quantitative rather than binary trait does not change our overall conclusions.

INTRODUCTION

Cancer is a heterogeneous collection of diseases with a wide variety of outcomes, natural histories and responses to therapy (Fidler 2012; Melo et al. 2013; Chen et al. 2014; Linnekamp et al. 2015; Shoag and Barbieri 2016; Kossaï et al. 2017). Cancerous neoplasms are often comprised of a diverse amalgamation of normal and malignant cells. A defining feature of cancerous cells is that as they arise, divide, and proliferate uncontrollably, they adapt to their host environment through natural selection (Brown et al. 2023). Efforts to characterize the clonal evolutionary dynamics of cancer have been ongoing for decades (Farber 1990; Carreira et al. 2014; McFadden et al. 2014; Yu et al. 2014; Bhang et al. 2015; Jamal-Hanjani et al. 2017; Dang et al. 2020; Sandén et al. 2020; Huang et al. 2023). These include experimental investigation of cancer's cellular kinetics (growth and death rates) and characterization of genetic changes both during initial growth and following treatment. Cancer treatments such as immuno- and chemo-therapeutics pose a strong selective pressure on these populations of cells. Ideally, the effects of these drugs on cancer cell populations are strong enough to drive the cancer

cells to extinction, but it is common for these populations to evolve resistance to treatment and then resume uncontrolled growth (Wagle et al. 2011; Finn et al. 2012; Awad et al. 2021; Priest et al. 2023). Resistance to therapy thus represents a major obstacle to long-term therapy success in patients. A better understanding of the evolutionary processes of cancer cell populations could lead to therapies that better mitigate or even exploit adaptive responses to treatment (Labrie et al. 2022). Modeling studies have proved a useful route to improving our understanding of the dynamics of cancer initiation, growth, and response to therapy (Cristini et al. 2003; Mallet and De Pillis 2006; Gatenby et al. 2007; Jeon et al. 2010; Sottoriva et al. 2010; Cook et al. 2016; Zangooei and Habibi 2017) and evolutionary models in particular can help us understand when and why some treatment strategies will fail, and also help inform new strategies (Mumenthaler et al. 2011; Beerenwinkel et al. 2015; Korobeinikov et al. 2017; Zhou et al. 2020; Pressley et al. 2021).

The interactions between a population and selective forces or environmental factors can be characterized through those evolutionary and ecological models that are applicable to cancer (reviewed in Merlo et al. 2006 and Laplane and Maley 2024) including the evolution of therapeutic resistance. For example, evolutionary rescue models (Gomulkiewicz and Holt 1995; Orr and Unckless 2008; Bell and Gonzalez 2009; Orr and Unckless 2014) define the patterns and dynamics of a population threatened with extinction due to a selective force and the probability that that population will avoid extinction and recover. This evolutionary rescue occurs when a population is being driven towards extinction by some selective pressure, but then a beneficial allele (or combination thereof) that is sufficient to overcome this selective pressure becomes common in the population soon enough so that the population can rebound before extinction. This results in a U-shaped trajectory of population size that is the hallmark of evolutionary rescue: initial rapid decline to a nadir, followed by renewed expansion (Orr and Unckless 2014).

Devising treatment strategies with sustained effectiveness is in essence finding ways to prevent evolutionary rescue. In cancer, the population consists of the tumor cells, the selective force driving the population towards extinction is the therapy, and the beneficial allele is the mutation that confers drug resistance. Whether a tumor cell population that is declining due to treatment will rescue depends on the chance that a resistant clonal subpopulation is established soon enough to prevent extinction. This in turn depends on the size of the cancer cell population at the onset of treatment along with the rate at which the treatment kills cancer cells (which together determine how long it will take the cancer population to go extinct unless rescue occurs), and the mutation rate for resistance alleles, as higher mutation rates increase the probability that rescue will occur at any point in time. The presence of preexisting resistance mutations also increases the probability of evolutionary rescue (Orr and Unckless

2008). Thus, preventing evolutionary rescue demands therapeutic regimes that maximize the selection against non-resistant tumor cells, while minimizing or delaying mutational events that could give rise to resistance. For example, evolutionary rescue theory implies that combining multiple therapeutic drugs with independent modes of action can greatly improve patient outcomes because the rate of the appearance of cells resistant to each drug in the combination would typically be far lower than the mutation rate for resistance to a single drug. This notion is supported by the success of combination therapy in comparison to single therapy protocols (Labrie et al. 1993; Li et al. 2014; Mokhtari et al. 2017; Palmer and Sorger 2017; Fisusi and Akala 2019; Plana et al. 2022).

An alternative approach is “extinction therapy” (Gatenby et al. 2019; Gatenby et al. 2020; Gatenby and Brown 2020; Felder et al. 2021). Extinction therapy proposes that after a radical change in the environment resulting in a population crash, the population could be driven to extinction by a comparatively minor environmental perturbation that otherwise would not be a major threat. At the onset, extinction therapy resembles standard-of-care treatment: the most effective available therapy is initially used, continuing this treatment as long as it remains effective. Once the cancer cell population size has been dramatically reduced by the first-line treatment: a “second strike” is performed with a different drug that may be less effective but is sufficient to push the now-threatened cancer cell population to extinction. Evolutionary modeling has shown that this “two-strike” extinction therapy can be effective (Gatenby et al. 2020), presuming the second strike is not too early (before the population has shrunk enough to be threatened by a less-effective treatment) or too late (once the population has been rescued by resistance to the first treatment and recovered to a large enough size to survive the second treatment).

Evolutionary modeling can answer outstanding fundamental questions about the conditions under which extinction therapy would be a superior approach, and how it should be carried out: How do factors like the mutation rate and the rate at which a therapy kills cancer cells influence the probability that a two-strike treatment will achieve extinction? What is the optimal timing of the second strike? Perhaps most importantly, when will simultaneous combination therapy be more effective than a sequential two-strike therapy, and vice versa?

Using population genetic simulations, we investigate the optimal timing of the second strike in an extinction therapy treatment protocol and compare the probability of extinction achieved by this sequential two-strike therapy with that of combination therapy. Our simulation approach reveals: 1) interactions between the optimal timing of two-strike sequential therapy, the mutation rate, and the rate at which the drug kills cancer cells; 2) the scenarios in which combination therapy outperforms optimally timed sequential extinction therapy and vice-versa, and 3) the implications of the genetic

architecture of resistance (i.e., a binary trait caused by a single mutation vs. a quantitative trait resulting from the cumulative effect of many mutations) for the optimal timing and effectiveness of a second strike.

METHODS

Several approaches have been developed and used to model the growth, response to therapy, and clonal evolution of cancer. These include mathematical models (Dingli et al. 2006; Benzekry et al. 2014; Sun and Hu 2018; Zhang et al. 2022), spatial models (Thalhauser et al. 2010; Komarova 2013; Waclaw et al. 2015), and agent-based models (Wang et al. 2007; Zhang et al. 2009; Mustapha et al. 2016; Gong et al. 2017).

We used the software SLiM 4.0 (Haller and Messer 2023) to simulate a diploid clonal population of cells undergoing expansion, treatment with two drugs, and mutations that confer resistance to these drugs. This software allows for agent-based evolutionary simulations which are widely used in the field of population genetics and provide a great deal of flexibility in modeling the evolution of resistance with minimal mathematical assumptions. Cells in these simulations have a specified genome size in base pairs and the simulation has a set mutation rate per base pair per cell cycle. To model clonal evolutionary dynamics, we set the recombination rate to 0. Events in the simulation occur over discrete generations (called cycles in SLiM), with the following order of events sequentially taking place during each generation (Figure S1):

1. Replication of cells: Each cell initially undergoes mitotic replication, producing two daughter cells with the exact same genome (i.e. containing the same set of mutations) as the parent cell. Thus, the cancer cell population size doubles during this step.
2. Mutation: After cell division, each daughter cell may acquire new mutations that affect resistance to treatment (see step 3). Mutations can randomly occur at sites along the genome according to the mutation rate per base pair per cell cycle. If a mutation occurs, its type (e.g. conferring resistance to drug 1 vs. conferring resistance to drug 2) is determined according to a discrete probability distribution of mutation types, referred to as the draw rates. For instance, if the draw rates of two mutation types are (0.5, 0.5), then each mutation type is equally likely to be chosen.
3. Calculation of fitness costs: This step involves tallying the number of mutations in a cell and then calculating its fitness depending on the presence or absence of treatment during the current generation. Treatment reduces fitness, but resistance mutations can mitigate or eliminate this fitness cost. Cells may also die in the absence of treatment (“turnover”).

4. Death and survival: Next, the fitness costs incurred by each cell are used to calculate the probability of survival. At this step, each cell has a P_{surv} probability of surviving, while the remaining cells die and thus removed from the simulation. Thus, the population contracts during this step, and those cells that survive return to step one (replication) in the next cell cycle.

First model: two-strike extinction therapy in an evolutionary rescue model

The simulation begins with the expansion phase: a population starting with a single cell grows exponentially as described above until reaching a size of ~2^{20}. We note that this population size is much smaller than the number of cells found in a tumor, but simulating smaller populations can still be useful way of modeling the dynamics of larger populations (but see Dabi and Schrider 2024). Next comes the treatment phase, which consists of the application of the first drug for a specified number of time steps, followed by immediately switching to the second drug. The number of cell cycles during which the first drug is applied is referred to as the "second-strike lag time". Throughout the simulation, two types of mutations can occur: m1 and m2, which confer resistance to the first and second drugs, respectively. However, these mutations confer no fitness advantage during the expansion and thus evolve under purely random drift throughout this phase. Note that we did not allow back-mutations: once a cell has acquired a given resistance mutation, all its descendants will harbor that same resistance allele.

In this model, resistance is a binary trait, and resistant cells do not experience any reduction in survival due to treatment nor due to any fitness tradeoff associated with resistance. The magnitude of the effect of each drug on the survival of non-resistant cells ("dose") during its treatment application is specified. The equation governing survival probability during step 4 of each generation is as follows:

$$P_{surv} = (1 - r_{turnover}) \times \left(1 - dose_{drug_1} \times (1 - \mathbb{1}_{m1})\right) \times \left(1 - dose_{drug_2} \times (1 - \mathbb{1}_{m2})\right)$$

where:

$r_{turnover}$ is the turnover rate of cells. We set this to 0.20 for all simulations (i.e. 80% of cells survive in the absence of treatment)

$dose_{drug_1}$ is the dose of the first drug,

$dose_{drug_2}$ is the dose of the second drug,

$\mathbb{1}_{m1}$ is the indicator function that the cell has a mutation resistant to drug 1,

and $\mathbb{1}_{m2}$ is the indicator function that the cell has a mutation resistant to drug 2.

During the expansion phase, both drug doses are 0, meaning fitness is only governed by the turnover rate. Application of either drug entails setting its dose to a specified value >0 while the other drug's dose remains at 0. The effect of each drug's dose is to reduce the probability of survival, and the indicator resistance functions govern whether a cell will experience this reduction in survival probability. Note that we use the shorthand "drug" to refer to each treatment, but each of these treatments could themselves be thought of as a combination of multiple drugs that together kills cancer cells according to the specified dose parameter and to which resistance evolves at the specified mutation rate.

We note that this simulation model differs from that of Gatenby et al.'s (2020) extinction therapy simulations in several key respects: 1) We model the two strikes in the same manner in that they are continually applied drugs that each reduce the fitness of cancer cells, while Gatenby et al. modeled the second strike as an instantaneous 40% reduction in the cancer cell population size rather than a continually applied treatment; 2) We end treatment with the first drug at the moment the second strike begins, whereas Gatenby et al.'s model continues therapy 1 after the second strike 3) Gatenby et al. modeled resistance as a quantitative rather than binary trait (a change we experiment with below); and 4) Gatenby et al.'s model includes an Allee effect, while ours does not.

For our first set of simulations, we varied the mutation rate and second-strike lag time to test the effect these parameters on the success of treatment. We tested per-base pair mutation rates between 1.0×10^{-6} and 3.1×10^{-5} with increments of 2×10^{-6} and second-strike lags between 1 and 20 cell cycles with increments of 1 cell cycle. Our drug dose effects in these simulations were fixed at 0.75 for both drugs (i.e. 75% of sensitive cells are killed by the drug each generation, on average). We ran 100 replicates of each parameter combination and measured the fraction of replicates in which the population went extinct, which we refer to as the "fraction of extinct replicates." We also tested the effect of using a lower dose of either drug across the various mutation rates. Furthermore, we fixed the mutation rate and examined the effect of varying both drug doses simultaneously.

Fixed trajectories simulations

In addition to examining sets of independent simulation replicates, we also conducted an *in silico* trial examining how outcomes of two-strike extinction therapy differed among a set of 55 *in silico* patients (with each patient defined by a combination of mutation rate and drug dose). Specifically, under a variant of our first model, we examined the dynamics leading to extinction or evolutionary rescue for each patient by fixing the trajectory of the population up to the time of applying the second treatment—this was

achieved by using a fixed initial random seed that was unique to that patient. Therefore, all replicates of patient share not only the drug dose and mutation rate, but the entire population trajectory up until the second treatment, including all birth and death events and mutations. When the second strike happens, a new replicate-specific random seed is chosen, producing stochastic trajectories after the second strike and allowing us to examine the distribution of treatment outcomes for each lag time for each synthetic patient.

Second model: the effect of combination therapy

We compared a combination therapy consisting of the simultaneous application of both drugs to sequential two-strike extinction therapy, again considering a range of second-strike lag times for the latter. In these simulations, combination therapy is simulated as both drugs having constant doses higher than 0 throughout the treatment phase. The dose effects of both drugs in these simulations are always equal, and the lowest dose used for each drug in the combination was 0.4. We note that when both drug doses are 0.4, the survival probability of cells is still below 0.5 (see survival probability formula in Methods), meaning that a net decrease in population size is expected in the absence of resistance. For the two-strike simulations included in this comparison, we fix the dose effect of both drugs to 0.9, while varying this dose effect during combination therapy. We ran 100 replicates of each parameter combination.

Third model: cross-resistance

We modified the second model to include a third rare mutation type which confers resistance to both drugs. The draw rates for m1, m2, and m3 mutations under this third model are 45%, 45%, and 10% respectively. The survival probability under this model is:

$$P_{surv} = (1 - r_{turnover}) \times \left(1 - dose_{drug_1} \times (1 - \mathbb{1}_{m1})\right) \times \left(1 - \mathbb{1}_{m3} \times strength_{cross_resistance}\right) \times \left(1 - dose_{drug_2} \times (1 - \mathbb{1}_{m2})\right) \times \left(1 - \mathbb{1}_{m3} \times strength_{cross_resistance}\right)$$

This equation shows that the presence of cross-resistance mutations (i.e. $\mathbb{1}_{m3} = 1$) dampens the effect of both drugs on fitness in proportion to the strength of the cross-resistance. Here, a cell that lacks a mutation of type m1 or m2 can still be resistant to both drugs if it has a mutation of type m3, but rather than full resistance, the degree of resistance imparted by this mutation is determined by $strength_{cross_resistance}$; if $strength_{cross_resistance} = 0$ then m3 provides no resistance, but if

$strength_{cross_resistance} = 1$ then m3 confers full resistance to both drugs. We ran these simulations across a range of values of $strength_{cross_resistance}$, comparing the outcomes of combination therapy to sequential therapy with various lag times.

Fourth model: varying drug doses and the mutation rate ratio in combination therapy

To investigate whether the optimal combination of doses during combination therapy depends on the relative rates of mutation to resistance alleles for the two drugs, we carried out simulations with varying ratios of the rates of m1 and m2 mutations (achieved by varying the rate of m1 mutations while fixing the rate of m2 mutations. Specifically, the mutation rate m1 mutations raged from 1×10^{-5} to $1.01 \times e^{-3}$ while the rate for m2 mutations was fixed to 1.5×10^{-5}. We also varied the ratio of the doses of the two drugs, under the constraint that $\left(1 - dose_{drug_1}\right) \times \left(1 - dose_{drug_2}\right)$ is fixed at 0.25. This was done by setting $dose_{drug_1}$ to a value between 0.30 and 0.70 and then setting $dose_{dru2}$ as follows:

$$dose_{drug_2} = 1 - 0.25/(1 - dose_{drug_1})$$

This ensures that the probability of survival for non-resistant cells is the same across all parameter combinations for this model, and thus that any differences in extinction probability across parameterizations are due to the interplay between drug mutation rates and drug doses.

Simulations modeling resistance as a quantitative trait

We also experimented with a model where drug resistance is a quantitative trait (Gomulkiewicz and Holt 1995). Cells can accumulate mutations conferring resistance to either drug, and each mutation contributes some amount to resistance against the corresponding drug that is drawn from a lognormal distribution. The parameters of this distribution were chosen so that the average resistance effect of a new mutation was 0.1, meaning that, on average, 10 accumulated mutations of a specific type should confer full resistance to the corresponding drug. This yielded a mean of -2.42759 and a standard deviation of 0.5. The survival equation then becomes:

$$P_{surv} = (1 - r_{turnover}) \times \left(1 - dose_{drug_1} \times \left(1 - \sum_i W_{m1,i}\right)\right) \times \left(1 - dose_{drug_2} \times \left(1 - \sum_i W_{m2,i}\right)\right)$$

where:

$r_{turnover}$, $dose_{drug_1}$, and $dose_{drug_2}$ are as defined above,

$W_{m1,i}$ is the fitness effect of the m1 mutation at i (zero if no such mutation present),

and $W_{m2,i}$ is the fitness effect of the m1 mutation at i, if present. Thus, $\sum_i W_{m1,i}$ and $\sum_i W_{m2,i}$ represent the cell's total amount of resistance to drugs 1 and 2, respectively

Note that under this model mutations can only increase resistance, and the combined effect of all resistance mutations in a genome was capped at 1.

RESULTS

Progression after treatment is a case of evolutionary rescue

Typical cancer treatment involves the application of the maximum tolerated dose (MTD) of a first-line therapy until either the cancer is eradicated or until progression is observed (Kareva et al. 2015). Progression often occurs because of the emergence of treatment-resistant cells within the cancer cell population, which quickly propagate until the remaining cells in the population are resistant to the treatment rendering it ineffective. This is an example of evolutionary rescue, wherein a population is rapidly crashing because of a change in the selective environment (i.e. treatment), but one or more resistance-conferring mutations become common enough in the population prior to extinction, thereby allowing the population to recover and eventually progress beyond the size observed before treatment. A typical example of the trajectory of a population undergoing evolutionary rescue is shown in Figure 1. In this example, the population size is initially growing exponentially, but then rapidly declines following the application of treatment. Eventually, the population size decreases to such a low level that it may not even be detectable. However, when the population is approaching its nadir, a subpopulation of resistant cells emerges and begins to become more prevalent, ensuring that the treatment will not succeed in eradicating the cancer. Below we explore alternative treatment strategies that are designed to reduce the probability of evolutionary rescue of the cancer cell population.

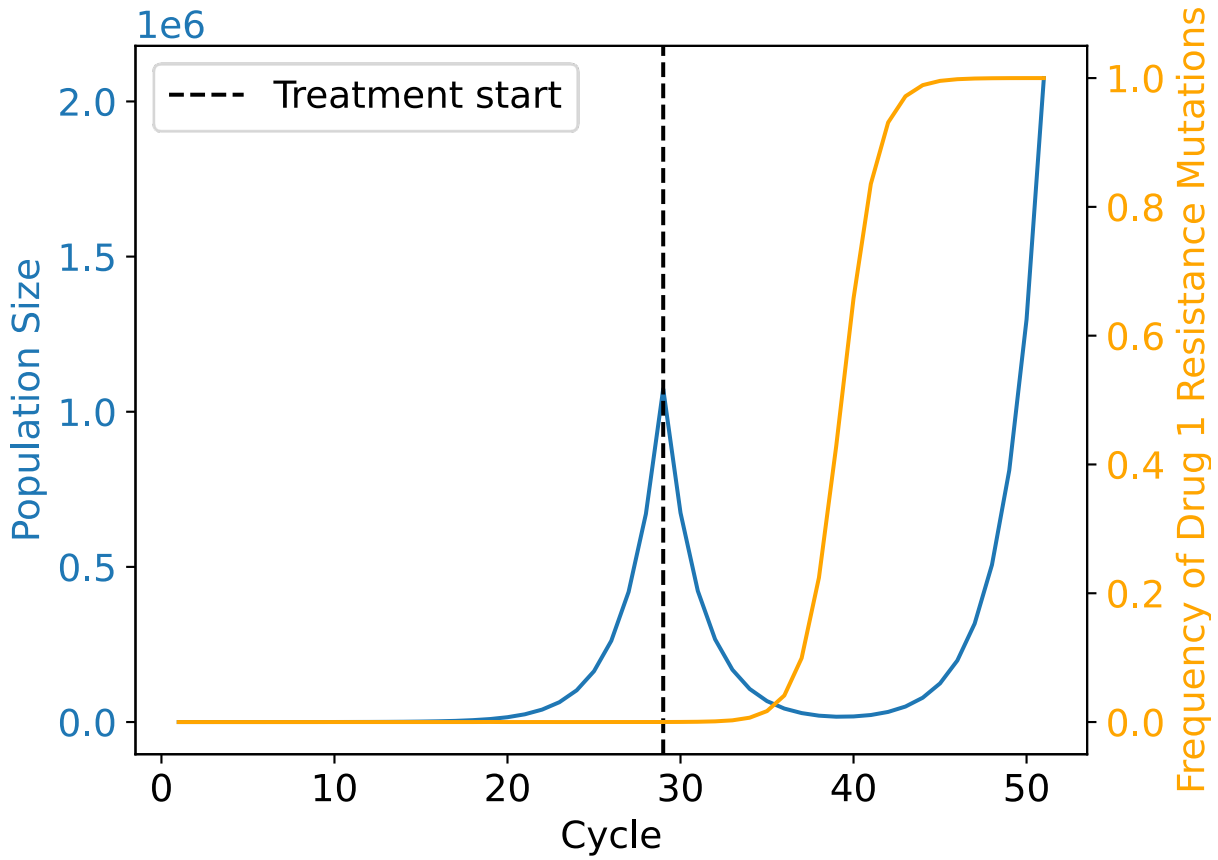

Figure 1. Trajectory of a cancer cell population undergoing evolutionary rescue following treatment. The population expands exponentially (blue line) until the first strike (dashed black line), after which the population declines rapidly. However, even as the population is declining, a resistance mutation has emerged and begun to increase in frequency in the population. As the treatment continues, the frequency of the resistance mutation continues to increase (orange line), the population eventually becomes fully resistant, resumes its exponential expansion, and ultimately recovers and progresses beyond its initial size pre-treatment. This trajectory is taken from a single simulation replicate of our first model (Methods), but without the application of a second strike. For this replicate the mutation rate was set to 1.5×10^{-5} and the drug dose to 0.66.

The optimal second-strike lag is independent of the mutation rate

In a two-strike cancer treatment scenario, the timing of the change from the first-line to the second-line therapy may have a profound effect on treatment success (Gatenby et al. 2020). To elucidate the relationship between the timing of the second-strike (the "second strike lag time") and the probability that the cancer cell population will be successfully driven to extinction, we used simulations to estimate the probability of extinction across second strike lag times and different rates of mutation to treatment-resistance alleles. Our results (Figure 2A) demonstrate that there exists an optimal lag

time between the onset of the first and second strikes for maximizing probability of inducing the extinction of the cell population. In general, the probability of extinction is low when the second drug is applied immediately following the application of the first (a lag time of only 1 cell cycle), then increases with greater lag times until an optimum is reached, and then decreases with increasing lag time. While there is no clear relationship between the mutation rate and the optimal lag time (Figure 2B), which remains generally between 7 and 9 cell cycles in our model, the mutation rate does exert an effect on the dynamics of population extinction probabilities across lag times. For instance, at lower mutation rates the extinction probability exhibits a broad plateau around the optimal lag time, implying that missing the optimal lag time is somewhat forgiving when resistance alleles do not frequently arise. As the mutation rate increases, however, the difference in extinction probability between the optimal lag time and suboptimal becomes starker, with a sharp peak around the optimum, and the extinction probability is also lower in general for all lag times.

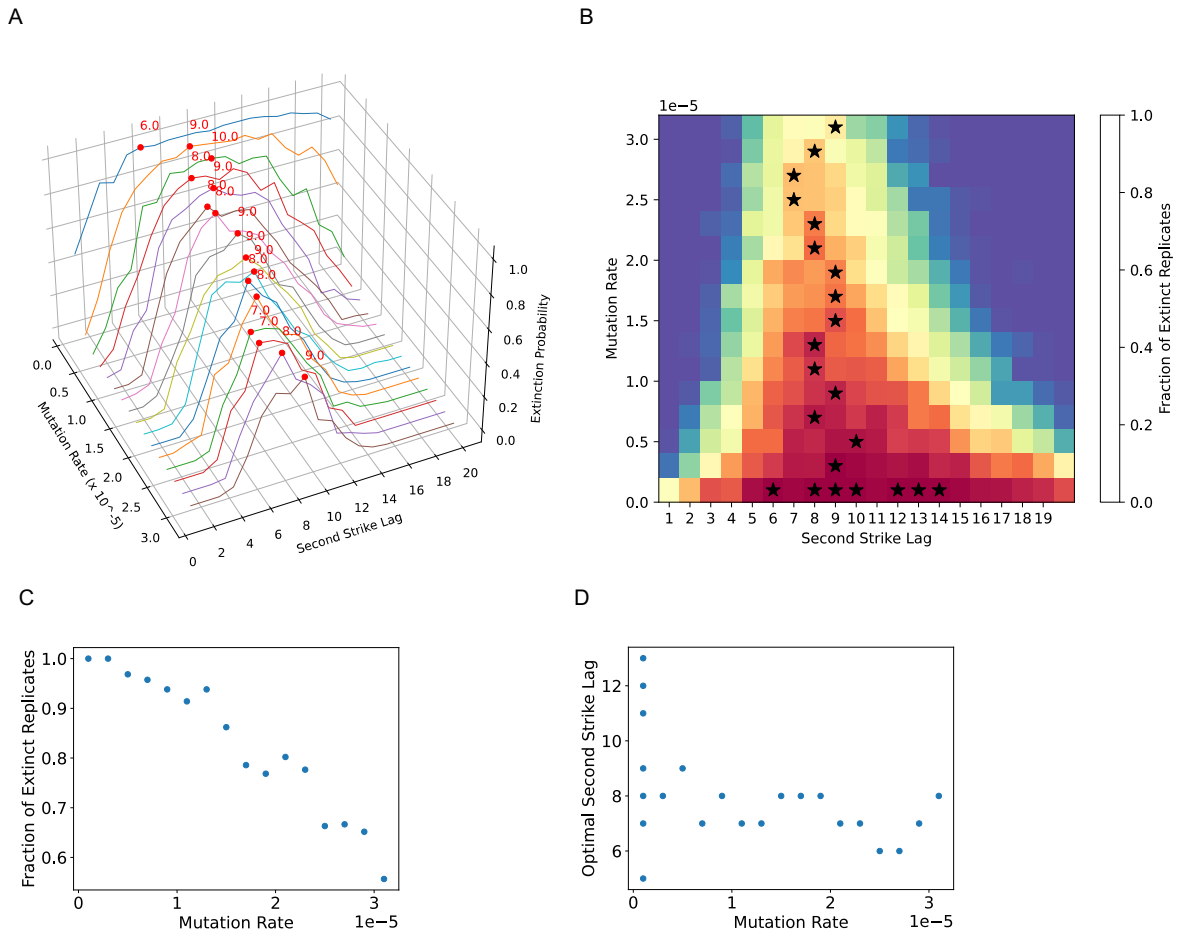

Figure 2. Extinction probability with varying mutation rates and second-strike lag times. A) Extinction rate vs mutation rate and lag time. The *x*-axis represents the per base pair mutation rate of resistant mutations. The *y*-axis (Second Strike Lag) represents the time spent under the first treatment before switching to the second treatment. The *z*-axis (Extinction Probability) represents the fraction of replicates where the population reached extinction. Red dots indicate the optimal lag time for each mutation rate (i.e. the lag time with the highest fraction of extinct replicates). The optimal lag time is relatively invariant across mutation rates. However, as the mutation rate increases, the difference in the extinction probability between the optimal lag time and other lag times becomes starker, and the extinction probability decreases for all lag times. B) Alternative representation of the results with color indicating the extinction probability estimate and black stars at the optimal lag time(s) for each mutation rate—multiple stars are drawn in the case of a tie. C) Per base pair mutation rate vs the extinction probability at the optimal lag time for that mutation rate. D) Optimal second-strike lag vs mutation rate. This represents a 2D projection of the points indicated by the red dots in A.

More effective therapeutics should be used first during extinction therapy

The rate at which a population is being driven to extinction is a key determinant of the probability and timing of evolutionary rescue (Orr and Unckless 2008, 2014). We examined the effect of our drug dose parameters on extinction probability and optimal

lag times by testing a scenario with a lower dose of drug 1 than drug 2, and one with a lower dose of drug 2 than drug 1. When the first drug has a dose of 0.65 and the second a dose of 0.75, the optimal lag time shifts to around 10 generations (Figure 3A), versus 7–9 generations in the equal-dose effect scenario shown in Figure 2. This increase is likely due to the increased time required to shrink the population of cells enough for the second strike to result in extinction. Furthermore, the mutation rate again appears to have little effect on this optimal lag time, and extinction probabilities are lower for all mutation rates compared to the case where both drugs have a dose of 0.75.

Next, we examined the case where the first drug has a higher dose (0.75) than the second (0.65)—a scenario is more relevant to standard-of-care and to current thinking about extinction therapy (Gatenby et al. 2019) in that the drug that kills cancer cells at a higher rate is used as the first-line treatment. We found that optimal lag times in this scenario resemble those of the case in which both drugs had an equal dose of 0.75 and are also not dependent on mutation rate. However, the extinction probabilities across all mutation rates are higher compared to the case of the first drug having the lower dose (Figure 3B vs Figure 3A). For instance, at a mutation rate of 1.5×10^{-5}, simulations where both drugs have a dose of 0.75 result in an extinction probability of ~0.86 at an optimal lag time of 8, but this decreases ~0.53 when the first drug has a lower dose effect (in this case, at an optimal lag time of 11); on the other hand, reducing the dose effect of the second drug but not the first has hardly any effect on the outcome (extinction probability of ~0.85, again with an optimal lag of 8). It is likely that the higher optimal lag time necessary to sufficiently reduce the population size when the first drug has a weaker effect also results in a higher likelihood of resistant mutants appearing. Thus, our results suggest using the stronger drug as the first strike during extinction therapy will provide the best chance of eradicating the cancer cell population.

Finally, we set the two drug doses equal to be one another and examined extinction dynamics across various dose values (with the mutation rate set to 1.5×10^{-5} in each instance). When the dose of both drugs is equal, the optimal time appears to increase as the drug dose decreases, and the extinction probability decreases from ~100% at a drug dose of 0.95 to ~20% at a drug dose of 0.60 (Figure 3C).

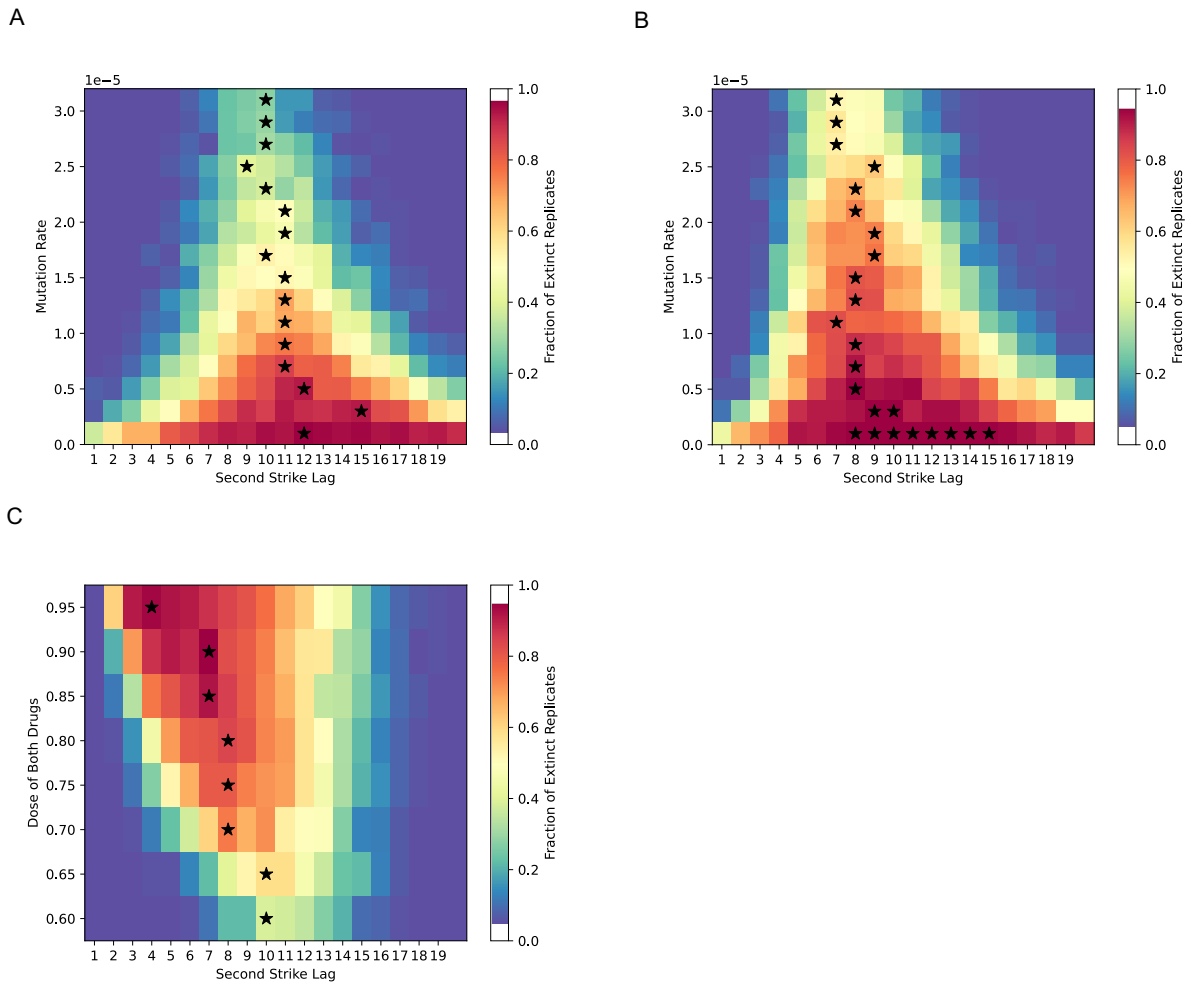

Figure 3. Extinction probability with varying drug doses and mutation rate. A) Extinction probability vs mutation rate and lag time when drug 1 has a lower dose (0.65) before switching to a second drug with a higher dose (0.75). B) Extinction probability vs mutation rate and lag time when the first drug has a higher dose (0.75) followed by treatment with a second drug with a lower dose (0.65). D) Extinction probability vs lag time and the dose of both drugs when the mutation rate is fixed at 1.5×10^{-5}, with the dose always being equal for both drugs. Black stars represent the optimal lag time(s) at each mutation rate.

Investigating the dynamics of evolutionary rescue in extinction therapy via *in silico* trials

Extinction therapy succeeds when the first strike removes variants that confer resistance to the second strike

Our simulation approach allows us to go a step further and ask, for a given patient's disease course, what would have been the optimal treatment strategy? Such information would not only improve our understanding of the dynamics impacting the probability of extinction, but also help us assess the potential of treatment strategies

422 tailored to individual patients. To this end, we conducted an *in silico* trail with a set of
423 patients receiving two-strike extinction therapy, and determined, for each specific
424 patient, the optimal lag time. This may differ from patient to patient both because of
425 different parameter values (e.g. mutation rates and drug effectiveness may differ across
426 patients) and because of stochasticity in the timing of the emergence of resistance and
427 other random events occurring both before and during the treatment course.

428 Our trial consisted of a set of 50 *in silico* patients, each of whom experienced a
429 deterministic disease trajectory up until the start of the second strike, at which point we
430 performed a set of 100 stochastic simulations to observe that patient's distribution of
431 outcomes for a given lag time (Methods). The results for some illustrative example
432 patients are shown in Figure 4, and the remainder are available on our project's GitHub
433 repository. An examination of these results reveals that two different, but related factors
434 govern the probability of treatment success (i.e. the fraction of extinct replicates) for a
435 given lag time. The first is the size of the cancer cell population at the time of the
436 second strike, and second is the frequency of the mutations at that time—results that
437 are consistent with analytical results (Orr and Unckless 2008). We therefore might
438 expect the optimal lag time to be the moment the population size is at its minimum (t_{min}),
439 and indeed in many cases we see that the extinction probability peaks when the second
440 strike begins at t_{min}. Two such examples are shown in Figure 4C and 4D; for these two
441 synthetic patients a plateau of extinction probability begins when the second strike
442 starts at t_{min}. However, in some cases there is standing variation for resistance to the
443 second treatment—these resistance mutations typically emerge during the expansion
444 phase and segregate at low frequency—that remains present in the population at t_{min}. In
445 those cases, continuing the first treatment for one or more cycles beyond t_{min} may
446 reduce the frequency of or even eliminate these resistance mutants from the population.
447 This is because cells that are resistant to the first treatment are selected for at the
448 expense of other genotypes, including those that have preexisting resistance to the
449 second treatment (e.g. Figures 4A, B).

450 <u>In silico *trials inform strategies for timing the second strike*</u>

451 The results of these synthetic trials can inform two-strike treatment strategies that are
452 more likely to prevent evolutionary rescue of the cancer cell population. For example,
453 when examining the results for all 55 synthetic patients, we find that switching to the
454 second treatment at the time where the population is at or near its minimum after the
455 first strike is generally a successful strategy (e.g. when the cancer cells' mutation rate is
456 set to 6×10^{-6}, the strategy of beginning the second strike at t_{min} results in an extinction
457 probability that is within 3% of its maximum for ~70% of synthetic patients).

458 However, in practice it may not be possible to known t_{min}, until after the
459 population has begun to rebound. We therefore assessed the effectiveness of beginning

460 the second strike after some amount of time/growth after t_{min} is observed. First, we
461 assessed the effectiveness of beginning the second strike when the cell population has
462 grown either 10%, 50%, or 150% larger than its minimum size following application of
463 the first strike. This generally results in a high extinction probability (Figure 4E), but this
464 probability decreases from >90% to ~80% as the amount of growth post-t_{min} before the
465 second strike increases from 10% to 150%); the variance in outcomes also increases
466 with the amount of lag time post-t_{min}. Similarly, if applying the second strike after a
467 specific number of cycles (i.e. 2, 3, or 4 cycles) after t_{min} again yields generally good
468 results (Figure 4F), although again efficacy decreases and outcome variability increases
469 as the amount of post-t_{min} lag time before the second strike increases. In summary, our
470 results suggest that while there may be variation in outcomes from patient to patient, a
471 second strike is most likely to be successful if it can be initiated at or shortly after t_{min}.

472

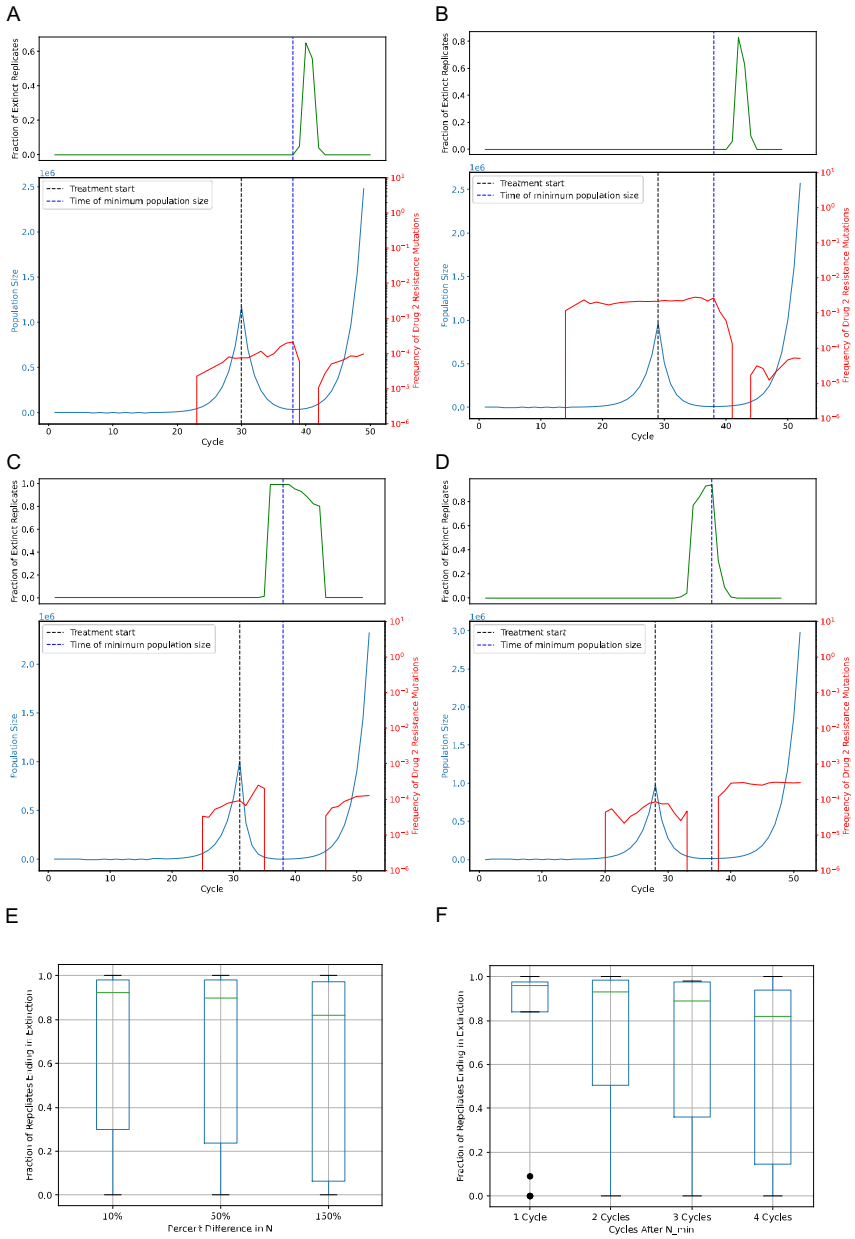

Figure 4. Example trajectories of synthetic patients with a mutation rate of 6×10^{-6}. A-B) Trajectories of synthetic patients where the optimal lag time occurs after the time of minimum population size (dashed blue vertical line) due to remaining standing variation that confers resistance to the second treatment. C-D) Trajectories of synthetic patients where the optimal lag time is at the population minimum because standing variation that confers resistance to the second treatment has been wiped out prior to the population reaching its minimum. Blue lines represent the population size, red line represent the frequency of the mutation conferring resistance to the second strike, and green lines in the upper sub-panels represent the fraction of replicates that have undergone extinction when switching to the second strike at that time. Results for the remaining 46 in silico patients are available on our GitHub repository. E) The distribution of extinction probabilities for a separate set of validation patients across three different timing strategies for the second strike; each value on the *x*-axis shows the percent growth in population size over the size of the minimum population during the first strike that is observed before applying the

second strike. F) The distribution of extinction probabilities for the set of validation patients across three more timing strategies for the second strike; each value on the *x*-axis shows the number of cycles after reaching the minimum population during the first strike before applying the second strike.

Combination therapy outperforms sequential therapy, except when cross-resistance is present

To compare the efficacy of combination therapy to optimally timed sequential therapy, we carried out simulations similar to those of the sequential therapy scenario above, but also included the possibility of combination therapy, wherein both drugs are applied simultaneously and at an equal dose until population rescue or extinction. We compared these simulations in the presence and absence of the possibility of mutations conferring cross-resistance to both drugs. Our results (Figure 5A) indicate that in the absence of cross-resistance combination therapy outperforms optimally timed sequential therapy for all combination drug doses above 0.4, with combination therapy failing to achieve extinction for any replicates when the dose of both drugs is 0.4. Furthermore, we note for all cases where the combination therapy dose is >0.40, the extinction probability does not increase substantially with the combination drug dose, regardless of the mutation rate. Indeed, it is worth stressing that the combination therapy outperforms two-strike extinction therapy even though in most of these parameterizations the individual drugs used in the two-strike therapy kill cancer cells at a much higher rate than the combined effect of the drugs in the combination therapy. This implies that it is the much-reduced probability of independently evolving resistance to both drugs rather than an elevated rate of killing cancer cells that is responsible for the greater efficacy of the combination therapy approach under this model.

When cross-resistance mutations are present and the mutation rate is sufficiently high (Figure 5B), optimally timed sequential therapy outperforms combination therapy when the combination dose drugs are at 0.45, at all the tested strengths of cross-resistance. We also note that both therapies fail to achieve the extinction of an appreciable fraction simulation replicates when the cross-resistance strength is especially high, and that this failure of treatment is more pronounced and occurs at even lower cross-resistance strengths when the mutation rate is 9×10^{-5} or higher. (See Figure S2 and Figure S3 for results at various mutation rates with and without cross-resistance). The lower probability of extinction under the sequential therapy at higher strengths of cross-resistance may be caused by cross-resistance mutations segregating at low frequency after the administration of the first drug (because the selective advantage of drug 1-resistance mutations over cross-resistance mutations is diminished), resulting in preexisting resistance to the second drug at the time of the switch in treatments.

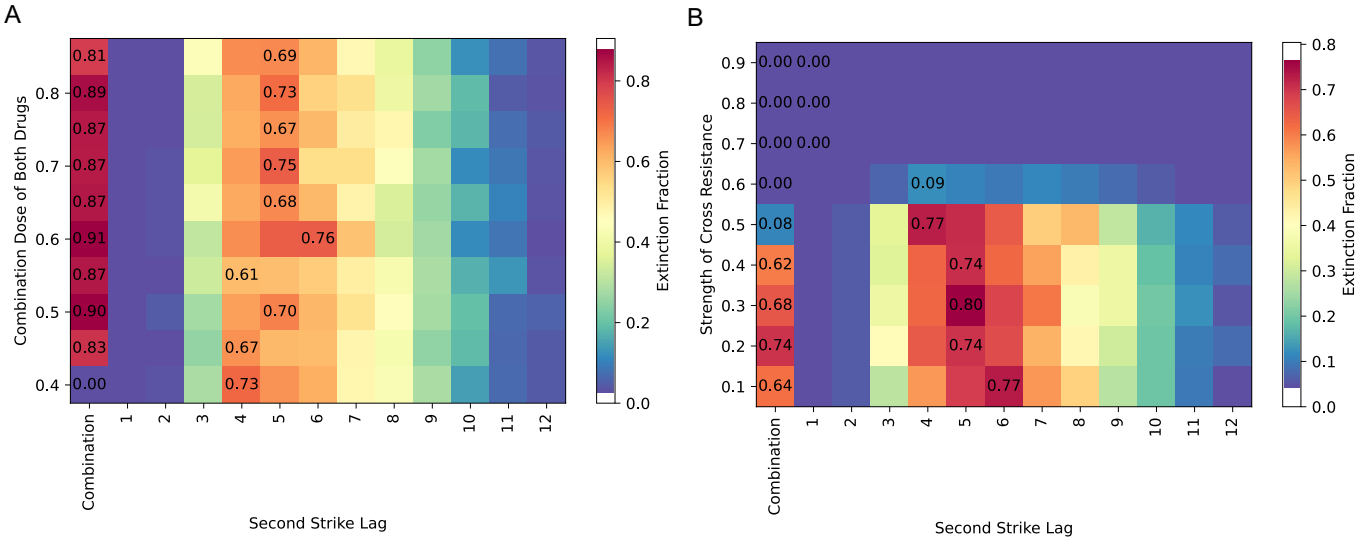

Figure 5. Comparison of efficacy between combination therapy and sequential therapy in the presence and absence of cross-resistance mutations. A) Combination therapy and sequential therapy at a mutation rate of 5×10^{-5} in the absence of cross-resistance at various doses of combination drug. The sequential drug doses are fixed at 0.95 for both drugs. B) Combination therapy and sequential therapy at a mutation rate of 5×10^{-5} at various strengths of cross-resistance; the combination drug doses being fixed at 0.45 and the sequential drug doses are fixed at 0.95 for both drugs. The fraction of extinct replicates for the for the sequential protocol at the optimal time and for the combination protocol are indicated in black text. Combination therapy outperforms optimally timed sequential therapy at all doses of combination drugs, while sequential therapy outperforms combination therapy at the selected dose in the presence of cross mutations regardless of the strength of cross-resistance.

Equal drug doses in combination therapy is optimal regardless of resistance mutation rates

Given the importance of the mutation rate to combination therapy efficacy, we sought to test whether there is an optimal ratio of drug doses during combination therapy if two resistant mutations have different mutation rates. To achieve this, we carried out simulations involving only combination therapy, fixing the mutation rate for resistance to the first drug and varying the mutation rate of resistance to the second drug. As outlined in the Methods, we varied the drug dose ratio but kept their combined effect constant so that the likelihood of death for treatment-sensitive cells was the same across all simulations. Our results (Figure S4) indicate that regardless of the difference in drug mutation rates, the highest chance of inducing population extinction is achieved when the doses of the two drugs in the combination is 1:1. Thus, our evolutionary rescue models suggests that it may be preferable to use a combination of treatments that each have a similar effect on the fitness of cancer cells.

551 **Extinction therapy dynamics appear largely similar if treatment resistance is a**
552 **quantitative trait**

553 So far, our simulations have treated resistance as a binary trait. In the following
554 simulations, we tested whether these results hold in scenarios where resistance is
555 conferred by the cumulative effect of multiple mutations. The contribution of each
556 mutation to resistance was drawn from a lognormal distribution as described in the
557 Methods. We find that an optimal lag time still exists in these simulations, and that it
558 remains independent of the mutation rate of resistance mutations (Figure S5A).
559 However, the peaks of extinction probability around the optimal lag times are not as
560 sharp as those in binary resistance simulations (compare to Figure 1).

561 We also examined the impact of varying drug doses under our under this
562 quantitative trait model, and made similar observations as under our binary trait model:
563 optimal lag times are independent of mutation rates regardless of which drug has a
564 lower dose, optimal lag times remain unchanged when drug 2 has the smaller dose, and
565 optimal lag times are higher and extinction probabilities are lower when drug 1 has the
566 smaller dose (Figure S5B, C, and D).

567

568 **DISCUSSION**

569 We performed forward-in-time agent-based population genetic simulations to evaluate
570 the effectiveness of several different treatment strategies under an evolutionary rescue
571 model. Our simulations of cancer cells evolving resistance under a sequential two-strike
572 "extinction therapy" regime, the timing of the switch from the first drug to the second has
573 a marked effect on the probability of the cell population going extinct (Figure 2). We also
574 find that using the more effective drug first and the less effective drug second leads to
575 substantially higher extinction probabilities than vice-versa (Figure 3). Furthermore, our
576 simulations show that combination therapy forms a formidable barrier to the evolution of
577 resistance when no mutations conferring cross-resistance exist, outperforming even
578 optimally timed sequential therapy involving much stronger drugs than those used in the
579 combination therapy (Figure 5A). This implies that combination therapies with lower
580 doses may be preferable to sequential therapy using drugs that achieve a higher kill
581 rate, because the probability of adapting to *each* drug in the combination is very low so
582 long as resistance mechanisms are independent—this result is consistent with insights
583 gained from studies of pest control and antimicrobial treatment strategies (Pimentel and
584 Burgess 1985; Angst et al. 2021). We note that another potential benefit of exploring
585 combinations of drugs that attack different targets in a tumor cell is that the time and
586 cost of developing and evaluating new treatments could be significantly reduced by
587 constructing a cocktail of existing pharmaceuticals rather than designing a new drug
588 (Mokhtari et al. 2017).

589 On the other hand, even drug combinations that target distinct parts of a cancer
590 cell can often be overcome through a single mechanism that produces multidrug
591 resistance such as elevated xenobiotic metabolism, increased growth factor production,
592 etc. (Luqmani 2005; Bukowski et al. 2020). Our simulations show that when it is
593 possible to acquire mutations that confer sufficient levels of cross-resistance,
594 combination therapy can yield worse outcomes than sequential therapy (Figure 5B).
595 The superior effectiveness of two-strike extinction therapy in this scenario is because, in
596 situations where cross-resistant mutations may be present but do not produce the same
597 level of resistance as mutations conferring resistance to a specific drug, the two-strike
598 therapy will cause single-drug resistance mutations to outcompete cross-resistant
599 mutations, leaving the population more vulnerable to the next drug in the sequence.
600 However, as the degree of resistance conferred by cross-resistance mutations
601 approaches that of the single-drug resistance mutations, the advantage of sequential
602 therapy is erased and both approaches fail with high probability. The failure of the two-
603 strike approach here is most likely a result of the persistence of segregating cross-
604 resistant variants following the application of the first drug which quickly render the
605 second strike ineffective. We also show that an equal dose for both drugs is always
606 optimal in combination therapy, regardless of whether resistance to one drug arises at a
607 higher rate than the other. Overall, our results emphasize the need for concerted efforts
608 to develop drug combinations that are recalcitrant to the evolution of multidrug
609 resistance (Pritchard et al. 2012), and suggest that when cross-resistance cannot be
610 avoided, two-strike extinction therapy strategies may yield better outcomes.

611 We used *in silico* patient trials to investigate the evolutionary dynamics of two-
612 strike extinction therapy in greater detail. While we found that for many patients the
613 optimal time to switch from the first to the second drug was at or near t_{min}, the time at
614 which the cancer cell population reaches its minimum and begins to rebound, this time
615 may differ substantially among patients. We do find that, if one switches treatments
616 shortly after t_{min}, the probability of extinction is often near its maximum (Figure 4).
617 However, we note that because the absolute amount of growth occurring immediately
618 after t_{min} is relatively minimal (Figure 1 and Figure 4), directly observing that t_{min} has
619 very recently been reached may not be feasible in practice, and thus if one waits until
620 observable progression to initiate the second strike it may already be too late. We
621 therefore argue that efforts to accurately predict t_{min} for a given patient based on a
622 limited number of scans/assays may prove to be a better route toward improving patient
623 outcomes.

624 Our *in silico* trials also clearly show how adaptation to a treatment can remove
625 diversity that could respond to a second treatment. Therefore, the success of two-strike
626 extinction therapy shares some similarity to the strategy of imposing an evolutionary
627 “double bind,” wherein resistance to one treatment confers susceptibility to another

628 (Gatenby, Brown, et al. 2009; Basanta et al. 2012) although in our case this is a side
629 effect of the reduction in tumor heterogeneity caused by selection rather than a direct
630 phenotypic cost of resistance. In other words, the benefit of the first treatment is not only
631 to shrink the size of the cancer cell population, but also to reduce the amount of
632 diversity that could allow the population to immediately adapt to the second strike
633 (Messer and Petrov 2013). If treatments are switched too early, mutations conferring
634 resistance to the second strike may remain present in the cell population, while waiting
635 too long allows the population to rebound and also allows mutations conferring
636 resistance to the second strike to randomly (re-)emerge in the population. Our results
637 also imply that the strategy of repeated changes of the selective environment (i.e.
638 treating a patient with a series of drugs used one after another in sequence), can be
639 further heighten the probability of extinction, consistent with evolutionary theory
640 suggesting that frequent or continual environmental change can drive even initially very
641 robust and adaptable populations to extinction (Bürger and Lynch 1995; Orive et al.
642 2019).

643 Finally, we show that the genetic architecture of resistance has implications for
644 the effectiveness of sequential therapy. Specifically, although we observed generally
645 similar dynamics whether treatment resistance is a binary trait or a quantitative trait
646 where the degree of resistance is proportional to the sum of the effects of multiple
647 mutations, in the latter scenario extinction probability displays broader plateaus around
648 the optimal lag times (Figure S5A). This may suggest that, all else being equal,
649 sequential therapy involving treatments that exert highly polygenic selection on cancer
650 populations may require less precision in timing the second strike in order to achieve
651 optimal outcomes, whereas treatments for which resistance is governed by a single
652 locus may in some cases yield poor outcomes even if the timing of the second strike
653 misses the optimum by a relatively small period of time (Figure 2).

654 Overall, our results suggest that consideration of the dynamics of evolutionary
655 rescue can inform optimal treatment strategies and timings. The simulation strategy that
656 we have adopted here is highly flexible and our code can be easily adapted to model
657 additional treatment strategies (e.g. adaptive therapy; Gatenby, Silva, et al. 2009;
658 Zhang et al. 2017; Zhang et al. 2022) and to incorporate additional complexity into our
659 model of cancer cell population evolution, adaptation, and extinction. Such features
660 could include but are not limited to spatial heterogeneity and dynamics (Schmelz et al.
661 2021; Noble et al. 2022; Seferbekova et al. 2023), Allee effects (Boukal and Berec
662 2002; Konstorum et al. 2016; Brown et al. 2017; Gerlee et al. 2022), treatment refugia
663 (Fu et al. 2015), non-genetic resistance mechanisms such as epigenetic responses
664 (Bell and Gilan 2020) and transitions to drug-tolerant cell states (Sharma et al. 2010;
665 Shaffer et al. 2017; Oren et al. 2021), and increasing rates of resistance mutations over
666 time resulting from increased genome instability (Lukow et al. 2021). More broadly, our

study demonstrates the potential of flexible forward population genetic simulations of evolutionary rescue scenarios for investigating the dynamics of diverse treatment/management strategies for cancer and other diseases/organisms where the emergence of resistance is a common occurrence (e.g. antibiotic resistance, pesticide resistance, etc). Our agent-based simulation model could be readily extended to investigate these phenomena as well, including in recombining organisms.

ACKNOWLEDGMENTS

The authors thank attendees of the Triangle Center for Evolutionary Medicine's 2023 Cancer and Evolution Catalysis Meeting for feedback on a preliminary version of this project.

FUNDING

DRS was supported by National Institutes of Health award R35GM138286, and AD was supported by the Royster Society of Fellows at the University of North Carolina at Chapel Hill.

DATA AVAILABILITY

All code necessary for conducting the simulations carried out in this study can be found at https://github.com/SchriderLab/cancer_sims.

REFERENCES

Angst DC, Tepekule B, Sun L, Bogos B, Bonhoeffer S. 2021. Comparing treatment strategies to reduce antibiotic resistance in an in vitro epidemiological setting. Proceedings of the National Academy of Sciences. 118(13):e2023467118. doi:10.1073/pnas.2023467118.

Awad MM, Liu S, Rybkin II, Arbour KC, Dilly J, Zhu VW, Johnson ML, Heist RS, Patil T, Riely GJ, et al. 2021. Acquired Resistance to KRASG12C Inhibition in Cancer. N Engl J Med. 384(25):2382–2393. doi:10.1056/NEJMoa2105281.

Basanta D, Gatenby RA, Anderson ARA. 2012. Exploiting Evolution To Treat Drug Resistance: Combination Therapy and the Double Bind. Mol Pharmaceutics. 9(4):914–921. doi:10.1021/mp200458e.

Beerenwinkel N, Schwarz RF, Gerstung M, Markowetz F. 2015. Cancer Evolution: Mathematical Models and Computational Inference. Systematic Biology. 64(1):e1–e25. doi:10.1093/sysbio/syu081.

Bell CC, Gilan O. 2020. Principles and mechanisms of non-genetic resistance in cancer. Br J Cancer. 122(4):465–472. doi:10.1038/s41416-019-0648-6.

Bell G, Gonzalez A. 2009. Evolutionary rescue can prevent extinction following environmental change. Ecol Lett. 12(9):942–948. doi:10.1111/j.1461-0248.2009.01350.x.

Benzekry S, Lamont C, Beheshti A, Tracz A, Ebos JML, Hlatky L, Hahnfeldt P. 2014. Classical Mathematical Models for Description and Prediction of Experimental Tumor Growth. PLOS Computational Biology. 10(8):e1003800. doi:10.1371/journal.pcbi.1003800.

Bhang HC, Ruddy DA, Krishnamurthy Radhakrishna V, Caushi JX, Zhao R, Hims MM, Singh AP, Kao I, Rakiec D, Shaw P, et al. 2015. Studying clonal dynamics in response to cancer therapy using high-complexity barcoding. Nat Med. 21(5):440–448. doi:10.1038/nm.3841.

Boukal DS, Berec L. 2002. Single-species models of the Allee effect: extinction boundaries, sex ratios and mate encounters. J Theor Biol. 218(3):375–394. doi:10.1006/jtbi.2002.3084.

Brown JS, Amend SR, Austin RH, Gatenby RA, Hammarlund EU, Pienta KJ. 2023. Updating the Definition of Cancer. Mol Cancer Res. 21(11):1142–1147. doi:10.1158/1541-7786.MCR-23-0411.

Brown JS, Cunningham JJ, Gatenby RA. 2017. Aggregation Effects and Population-Based Dynamics as a Source of Therapy Resistance in Cancer. IEEE Trans Biomed Eng. 64(3):512–518. doi:10.1109/TBME.2016.2623564.

Bukowski K, Kciuk M, Kontek R. 2020. Mechanisms of Multidrug Resistance in Cancer Chemotherapy. International Journal of Molecular Sciences. 21(9):3233. doi:10.3390/ijms21093233.

Bürger R, Lynch M. 1995. EVOLUTION AND EXTINCTION IN A CHANGING ENVIRONMENT: A QUANTITATIVE-GENETIC ANALYSIS. Evolution. 49(1):151–163. doi:10.1111/j.1558-5646.1995.tb05967.x.

Carreira S, Romanel A, Goodall J, Grist E, Ferraldeschi R, Miranda S, Prandi D, Lorente D, Frenel J-S, Pezaro C, et al. 2014. Tumor clone dynamics in lethal prostate cancer. Science Translational Medicine. 6(254):254ra125-254ra125. doi:10.1126/scitranslmed.3009448.

Chen Z, Fillmore CM, Hammerman PS, Kim CF, Wong K-K. 2014. Non-small-cell lung cancers: a heterogeneous set of diseases. Nat Rev Cancer. 14(8):535–546. doi:10.1038/nrc3775.

Cook LM, Araujo A, Pow-Sang JM, Budzevich MM, Basanta D, Lynch CC. 2016. Predictive computational modeling to define effective treatment strategies for bone metastatic prostate cancer. Sci Rep. 6(1):29384. doi:10.1038/srep29384.

Cristini V, Lowengrub J, Nie Q. 2003. Nonlinear simulation of tumor growth. J Math Biol. 46(3):191–224. doi:10.1007/s00285-002-0174-6.

Dabi A, Schrider DR. 2024 Nov 6. Population size rescaling significantly biases outcomes of forward-in-time population genetic simulations. Genetics.:iyae180. doi:10.1093/genetics/iyae180.

Dang HX, Krasnick BA, White BS, Grossman JG, Strand MS, Zhang J, Cabanski CR, Miller CA, Fulton RS, Goedegebuure SP, et al. 2020. The clonal evolution of metastatic colorectal cancer. Science Advances. 6(24):eaay9691. doi:10.1126/sciadv.aay9691.

Dingli D, Cascino MD, Josić K, Russell SJ, Bajzer Ž. 2006. Mathematical modeling of cancer radiovirotherapy. Mathematical Biosciences. 199(1):55–78. doi:10.1016/j.mbs.2005.11.001.

Farber E. 1990. Clonal adaptation during carcinogenesis. Biochemical Pharmacology. 39(12):1837–1846. doi:10.1016/0006-2952(90)90599-G.

Felder SI, Fleming JB, Gatenby RA. 2021. Treatment-induced evolutionary dynamics in nonmetastatic locally advanced rectal adenocarcinoma. Adv Cancer Res. 151:39–67. doi:10.1016/bs.acr.2021.02.003.

Fidler IJ. 2012. Biological heterogeneity of cancer. Human Vaccines & Immunotherapeutics. 8(8):1141–1142. doi:10.4161/hv.19643.

Finn L, Markovic SN, Joseph RW. 2012. Therapy for metastatic melanoma: the past, present, and future. BMC Med. 10:23. doi:10.1186/1741-7015-10-23.

Fisusi FA, Akala EO. 2019. Drug Combinations in Breast Cancer Therapy. Pharmaceutical Nanotechnology. 7(1):3–23. doi:10.2174/2211738507666190122111224.

Fu F, Nowak MA, Bonhoeffer S. 2015. Spatial Heterogeneity in Drug Concentrations Can Facilitate the Emergence of Resistance to Cancer Therapy. PLoS Comput Biol. 11(3):e1004142. doi:10.1371/journal.pcbi.1004142.

Gatenby RA, Artzy-Randrup Y, Epstein T, Reed DR, Brown JS. 2020. Eradicating Metastatic Cancer and the Eco-Evolutionary Dynamics of Anthropocene Extinctions. Cancer Res. 80(3):613–623. doi:10.1158/0008-5472.CAN-19-1941.

Gatenby RA, Brown J, Vincent T. 2009. Lessons from Applied Ecology: Cancer Control Using an Evolutionary Double Bind. Cancer Research. 69(19):7499–7502. doi:10.1158/0008-5472.CAN-09-1354.

Gatenby RA, Brown JS. 2020. Integrating evolutionary dynamics into cancer therapy. Nat Rev Clin Oncol. 17(11):675–686. doi:10.1038/s41571-020-0411-1.

Gatenby RA, Silva AS, Gillies RJ, Frieden BR. 2009. Adaptive therapy. Cancer Res. 69(11):4894–4903. doi:10.1158/0008-5472.CAN-08-3658.

Gatenby RA, Smallbone K, Maini PK, Rose F, Averill J, Nagle RB, Worrall L, Gillies RJ. 2007. Cellular adaptations to hypoxia and acidosis during somatic evolution of breast cancer. Br J Cancer. 97(5):646–653. doi:10.1038/sj.bjc.6603922.

Gatenby RA, Zhang J, Brown JS. 2019. First Strike–Second Strike Strategies in Metastatic Cancer: Lessons from the Evolutionary Dynamics of Extinction. Cancer Research. 79(13):3174–3177. doi:10.1158/0008-5472.CAN-19-0807.

Gerlee P, Altrock PM, Malik A, Krona C, Nelander S. 2022. Autocrine signaling can explain the emergence of Allee effects in cancer cell populations. PLoS Comput Biol. 18(3):e1009844. doi:10.1371/journal.pcbi.1009844.

Gomulkiewicz R, Holt RD. 1995. WHEN DOES EVOLUTION BY NATURAL SELECTION PREVENT EXTINCTION? Evolution. 49(1):201–207. doi:10.1111/j.1558-5646.1995.tb05971.x.

Gong C, Milberg O, Wang B, Vicini P, Narwal R, Roskos L, Popel AS. 2017. A computational multiscale agent-based model for simulating spatio-temporal tumour immune response to PD1 and PDL1 inhibition. Journal of The Royal Society Interface. 14(134):20170320. doi:10.1098/rsif.2017.0320.

Huang KK, Ma H, Chong RHH, Uchihara T, Lian BSX, Zhu F, Sheng T, Srivastava S, Tay ST, Sundar R, et al. 2023. Spatiotemporal genomic profiling of intestinal metaplasia reveals clonal dynamics of gastric cancer progression. Cancer Cell. 41(12):2019-2037.e8. doi:10.1016/j.ccell.2023.10.004.

Jamal-Hanjani M, Wilson GA, McGranahan N, Birkbak NJ, Watkins TBK, Veeriah S, Shafi S, Johnson DH, Mitter R, Rosenthal R, et al. 2017. Tracking the Evolution of Non–Small-Cell Lung Cancer. New England Journal of Medicine. 376(22):2109–2121. doi:10.1056/NEJMoa1616288.

Jeon J, Quaranta V, Cummings PT. 2010. An Off-Lattice Hybrid Discrete-Continuum Model of Tumor Growth and Invasion. Biophysical Journal. 98(1):37–47. doi:10.1016/j.bpj.2009.10.002.

Kareva I, Waxman DJ, Lakka Klement G. 2015. Metronomic chemotherapy: an attractive alternative to maximum tolerated dose therapy that can activate anti-tumor

immunity and minimize therapeutic resistance. Cancer Lett. 358(2):100–106. doi:10.1016/j.canlet.2014.12.039.

Komarova NL. 2013. Spatial stochastic models of cancer: Fitness, migration, invasion. MBE. 10(3):761–775. doi:10.3934/mbe.2013.10.761.

Konstorum A, Hillen T, Lowengrub J. 2016. Feedback Regulation in a Cancer Stem Cell Model can Cause an Allee Effect. Bull Math Biol. 78(4):754–785. doi:10.1007/s11538-016-0161-5.

Korobeinikov A, Starkov KE, Valle PA. 2017. Modeling cancer evolution: evolutionary escape under immune system control. J Phys: Conf Ser. 811(1):012004. doi:10.1088/1742-6596/811/1/012004.

Kossaï M, Leary A, Scoazec J-Y, Genestie C. 2017. Ovarian Cancer: A Heterogeneous Disease. Pathobiology. 85(1–2):41–49. doi:10.1159/000479006.

Labrie F, Belanger A, Simard J, Labrie C, Dupont A. 1993. Combination therapy for prostate cancer. Endocrine and biologic basis of its choice as new standard first-line therapy. Cancer. 71(S3):1059–1067. doi:10.1002/1097-0142(19930201)71:3+<1059::AID-CNCR2820711426>3.0.CO;2-6.

Labrie M, Brugge JS, Mills GB, Zervantonakis IK. 2022. Therapeutic opportunities created by adaptive responses to targeted therapies in cancer. Nat Rev Cancer. 22(6):323–339. doi:10.1038/s41568-022-00454-5.

Laplane L, Maley CC. 2024. The evolutionary theory of cancer: challenges and potential solutions. Nat Rev Cancer. 24(10):718–733. doi:10.1038/s41568-024-00734-2.

Li F, Zhao C, Wang L. 2014. Molecular-targeted agents combination therapy for cancer: Developments and potentials. International Journal of Cancer. 134(6):1257–1269. doi:10.1002/ijc.28261.

Linnekamp JF, Wang X, Medema JP, Vermeulen L. 2015. Colorectal Cancer Heterogeneity and Targeted Therapy: A Case for Molecular Disease Subtypes. Cancer Research. 75(2):245–249. doi:10.1158/0008-5472.CAN-14-2240.

Lukow DA, Sausville EL, Suri P, Chunduri NK, Wieland A, Leu J, Smith JC, Girish V, Kumar AA, Kendall J, et al. 2021. Chromosomal instability accelerates the evolution of resistance to anti-cancer therapies. Developmental Cell. 56(17):2427-2439.e4. doi:10.1016/j.devcel.2021.07.009.

Luqmani YA. 2005. Mechanisms of drug resistance in cancer chemotherapy. Med Princ Pract. 14 Suppl 1:35–48. doi:10.1159/000086183.

Mallet DG, De Pillis LG. 2006. A cellular automata model of tumor–immune system interactions. Journal of Theoretical Biology. 239(3):334–350. doi:10.1016/j.jtbi.2005.08.002.

841 McFadden DG, Papagiannakopoulos T, Taylor-Weiner A, Stewart C, Carter SL,
842 Cibulskis K, Bhutkar A, McKenna A, Dooley A, Vernon A, et al. 2014. Genetic and
843 Clonal Dissection of Murine Small Cell Lung Carcinoma Progression by Genome
844 Sequencing. Cell. 156(6):1298–1311. doi:10.1016/j.cell.2014.02.031.

845 Melo FDSE, Vermeulen L, Fessler E, Medema JP. 2013. Cancer heterogeneity—a
846 multifaceted view. EMBO reports. 14(8):686–695. doi:10.1038/embor.2013.92.

847 Merlo LMF, Pepper JW, Reid BJ, Maley CC. 2006. Cancer as an evolutionary and
848 ecological process. Nat Rev Cancer. 6(12):924–935. doi:10.1038/nrc2013.

849 Messer PW, Petrov DA. 2013. Population genomics of rapid adaptation by soft selective
850 sweeps. Trends in Ecology & Evolution. 28(11):659–669.
851 doi:10.1016/j.tree.2013.08.003.

852 Mokhtari RB, Homayouni TS, Baluch N, Morgatskaya E, Kumar S, Das B, Yeger H.
853 2017. Combination therapy in combating cancer. Oncotarget. 8(23):38022–38043.
854 doi:10.18632/oncotarget.16723.

855 Mumenthaler SM, Foo J, Leder K, Choi NC, Agus DB, Pao W, Mallick P, Michor F.
856 2011. Evolutionary modeling of combination treatment strategies to overcome
857 resistance to tyrosine kinase inhibitors in non-small cell lung cancer. Mol Pharm.
858 8(6):2069–2079. doi:10.1021/mp200270v.

859 Mustapha K, Gilli Q, Frayret J-M, Lahrichi N, Karimi E. 2016. Agent-based Simulation
860 Patient Model for Colon and Colorectal Cancer Care Trajectory. Procedia Computer
861 Science. 100:188–197. doi:10.1016/j.procs.2016.09.140.

862 Noble R, Burri D, Le Sueur C, Lemant J, Viossat Y, Kather JN, Beerenwinkel N. 2022.
863 Spatial structure governs the mode of tumour evolution. Nat Ecol Evol. 6(2):207–217.
864 doi:10.1038/s41559-021-01615-9.

865 Oren Y, Tsabar M, Cuoco MS, Amir-Zilberstein L, Cabanos HF, Hütter J-C, Hu B,
866 Thakore PI, Tabaka M, Fulco CP, et al. 2021. Cycling cancer persister cells arise from
867 lineages with distinct programs. Nature. 596(7873):576–582. doi:10.1038/s41586-021-
868 03796-6.

869 Orive ME, Holt RD, Barfield M. 2019. Evolutionary Rescue in a Linearly Changing
870 Environment: Limits on Predictability. Bull Math Biol. 81(11):4821–4839.
871 doi:10.1007/s11538-018-0504-5.

872 Orr HA, Unckless RL. 2008. Population extinction and the genetics of adaptation. Am
873 Nat. 172(2):160–169. doi:10.1086/589460.

874 Orr HA, Unckless RL. 2014. The Population Genetics of Evolutionary Rescue. PLOS
875 Genetics. 10(8):e1004551. doi:10.1371/journal.pgen.1004551.

Palmer AC, Sorger PK. 2017. Combination Cancer Therapy Can Confer Benefit via Patient-to-Patient Variability without Drug Additivity or Synergy. Cell. 171(7):1678-1691.e13. doi:10.1016/j.cell.2017.11.009.

Pimentel D, Burgess M. 1985. Effects of Single Versus Combinations of Insecticides on the Development of Resistance. Environmental Entomology. 14(5):582–589. doi:10.1093/ee/14.5.582.

Plana D, Palmer AC, Sorger PK. 2022. Independent Drug Action in Combination Therapy: Implications for Precision Oncology. Cancer Discovery. 12(3):606–624. doi:10.1158/2159-8290.CD-21-0212.

Pressley M, Salvioli M, Lewis DB, Richards CL, Brown JS, Staňková K. 2021. Evolutionary Dynamics of Treatment-Induced Resistance in Cancer Informs Understanding of Rapid Evolution in Natural Systems. Front Ecol Evol. 9. doi:10.3389/fevo.2021.681121. [accessed 2024 Nov 22]. https://www.frontiersin.org/journals/ecology-and-evolution/articles/10.3389/fevo.2021.681121/full.

Priest K, Le A, Gebregzabheir A, Nijmeh H, Reis GB, Mandell M, Davies KD, Lawrence C, O'Donnell E, Doebele RC, et al. 2023. Evolution of acquired resistance in a ROS1+ KRAS G12C+ NSCLC through the MAPK pathway. npj Precis Onc. 7(1):1–7. doi:10.1038/s41698-023-00349-0.

Pritchard JR, Lauffenburger DA, Hemann MT. 2012. Understanding resistance to combination chemotherapy. Drug Resistance Updates. 15(5):249–257. doi:10.1016/j.drup.2012.10.003.

Sandén C, Lilljebjörn H, Orsmark Pietras C, Henningsson R, Saba KH, Landberg N, Thorsson H, von Palffy S, Peña-Martinez P, Högberg C, et al. 2020. Clonal competition within complex evolutionary hierarchies shapes AML over time. Nat Commun. 11(1):579. doi:10.1038/s41467-019-14106-0.

Schmelz K, Toedling J, Huska M, Cwikla MC, Kruetzfeldt L-M, Proba J, Ambros PF, Ambros IM, Boral S, Lodrini M, et al. 2021. Spatial and temporal intratumour heterogeneity has potential consequences for single biopsy-based neuroblastoma treatment decisions. Nat Commun. 12(1):6804. doi:10.1038/s41467-021-26870-z.

Seferbekova Z, Lomakin A, Yates LR, Gerstung M. 2023. Spatial biology of cancer evolution. Nat Rev Genet. 24(5):295–313. doi:10.1038/s41576-022-00553-x.

Shaffer SM, Dunagin MC, Torborg SR, Torre EA, Emert B, Krepler C, Beqiri M, Sproesser K, Brafford PA, Xiao M, et al. 2017. Rare cell variability and drug-induced reprogramming as a mode of cancer drug resistance. Nature. 546(7658):431–435. doi:10.1038/nature22794.

Sharma SV, Lee DY, Li B, Quinlan MP, Takahashi F, Maheswaran S, McDermott U, Azizian N, Zou L, Fischbach MA, et al. 2010. A chromatin-mediated reversible drug-

tolerant state in cancer cell subpopulations. Cell. 141(1):69–80. doi:10.1016/j.cell.2010.02.027.

Shoag J, Barbieri CE. 2016. Clinical variability and molecular heterogeneity in prostate cancer. Asian Journal of Andrology. 18(4):543. doi:10.4103/1008-682X.178852.

Sottoriva A, Verhoeff JJC, Borovski T, McWeeney SK, Naumov L, Medema JP, Sloot PMA, Vermeulen L. 2010. Cancer Stem Cell Tumor Model Reveals Invasive Morphology and Increased Phenotypical Heterogeneity. Cancer Research. 70(1):46–56. doi:10.1158/0008-5472.CAN-09-3663.

Sun X, Hu B. 2018. Mathematical modeling and computational prediction of cancer drug resistance. Briefings in Bioinformatics. 19(6):1382–1399. doi:10.1093/bib/bbx065.

Thalhauser CJ, Lowengrub JS, Stupack D, Komarova NL. 2010. Selection in spatial stochastic models of cancer: Migration as a key modulator of fitness. Biol Direct. 5(1):21. doi:10.1186/1745-6150-5-21.

Waclaw B, Bozic I, Pittman ME, Hruban RH, Vogelstein B, Nowak MA. 2015. A spatial model predicts that dispersal and cell turnover limit intratumour heterogeneity. Nature. 525(7568):261–264. doi:10.1038/nature14971.

Wagle N, Emery C, Berger MF, Davis MJ, Sawyer A, Pochanard P, Kehoe SM, Johannessen CM, MacConaill LE, Hahn WC, et al. 2011. Dissecting Therapeutic Resistance to RAF Inhibition in Melanoma by Tumor Genomic Profiling. J Clin Oncol. 29(22):3085–3096. doi:10.1200/JCO.2010.33.2312.

Wang Z, Zhang L, Sagotsky J, Deisboeck TS. 2007. Simulating non-small cell lung cancer with a multiscale agent-based model. Theor Biol Med Model. 4(1):50. doi:10.1186/1742-4682-4-50.

Yu H, Han Z, Wang Y, Xin H. 2014. The Clonal Evolution and Therapeutic Approaches of Lung Cancer. Cell Biochem Biophys. 70(1):63–71. doi:10.1007/s12013-014-9910-y.

Zangooei MH, Habibi J. 2017. Hybrid multiscale modeling and prediction of cancer cell behavior. PLOS ONE. 12(8):e0183810. doi:10.1371/journal.pone.0183810.

Zhang J, Cunningham J, Brown J, Gatenby R. 2022. Evolution-based mathematical models significantly prolong response to abiraterone in metastatic castrate-resistant prostate cancer and identify strategies to further improve outcomes. Perry GH, editor. eLife. 11:e76284. doi:10.7554/eLife.76284.

Zhang J, Cunningham JJ, Brown JS, Gatenby RA. 2017. Integrating evolutionary dynamics into treatment of metastatic castrate-resistant prostate cancer. Nat Commun. 8(1):1816. doi:10.1038/s41467-017-01968-5.

Zhang L, Wang Z, Sagotsky JA, Deisboeck TS. 2009. Multiscale agent-based cancer modeling. J Math Biol. 58(4):545–559. doi:10.1007/s00285-008-0211-1.

Zhou J, Liu Y, Zhang Y, Li Q, Cao Y. 2020. Modeling Tumor Evolutionary Dynamics to Predict Clinical Outcomes for Patients with Metastatic Colorectal Cancer: A Retrospective Analysis. Cancer Res. 80(3):591–601. doi:10.1158/0008-5472.CAN-19-1940.